Magnetic irreversibility and saturation criteria in ultrasmall bi-magnetic nanoparticles

Rafael Cabreira Gomes, Franciscarlos G da Silva, Tatiane-Quetly Silva, Guilherme Gomide, Vanessa Pilati, Renata Aquino, Julian Geshev, Régine Perzynski, Jérôme Depeyrot

Version of Record: https://www.sciencedirect.com/science/article/pii/S0925838820300098
Manuscript_082707bc4ceb4f569b34e35ac1c9f0cd

Magnetic irreversibility and saturation criteria in ultrasmall bi-magnetic nanoparticles

Rafael Cabreira Gomes[a,b,d], Fransciscarlos G. da Silva[a,c,d], Tatiane Q. Muniz[c], Guilherme Gomide[c], Vanessa Pilati[c], Renata Aquino[a], Julian Geshev[e], Régine Perzynski[d], Jérôme Depeyrot[c]

[a] *Laboratory for Environmental and Applied Nanoscience - LNAA, Faculdade UnB Planaltina, Universidade de Brasília, 73345-010, Brasília, DF, Brazil*
[b] *Departamento de Física, Universidade Federal de Santa Catarina, 88040-900, Florianópolis, SC, Brazil*
[c] *Complex Fluids Group, Instituto de Física, Universidade de Brasília, Caixa Postal 04455, 70919-970, Brasília, DF, Brazil*
[d] *Sorbonne Université, CNRS, PHysico-chimie des Electrolytes et Nanosystémes InterfaciauX, F-75005, Paris, France*
[e] *Instituto de Física, Universidade Federal do Rio Grande do Sul, 91501-970 Porto Alegre, RS, Brazil*

Abstract

Ultrasmall magnetic particles are notorious for exhibiting a magnetization increase even at quite intense applied fields, behavior which can be interpreted as a non-saturation of the magnetic disordered shell even if the nanoparticle magnetization is reversible. In this work we study two kinds of ultrasmall core@shell nanoparticles (3 nm) with contrasting core anisotropy, composed of $MnFe_2O_4$ and $CoFe_2O_4$ cores covered by a thin maghemite layer. In order to investigate the saturation criterion associated to the closure of major loops (in contrast to minor loops), we use several procedures to determine, at moderate fields, if the effective anisotropy energy barrier is overcome or not. Firstly, we carefully evaluate the closure field of the hysteresis loop, interpreted as the effective anisotropy field, correspondent to two different contributions. One, arising from the nanoparticle core, is related to the coercivity and the other one is associated to pinned spins of the nanoparticle shell. Secondly, the ZFC-FC magnetization measurements taken at different fields give us information about both the anisotropy energy barrier distribution and the thermal dependence of effective anisotropy field. Thirdly, forced minor loops are performed, measured after either ZFC or FC processes, to counter-check the effective magnetic anisotropy at low temperature of both samples. Finally, we perform major hysteresis loop calculations in order to better understand the magnetization processes involved. To go further, we propose in this study a procedure to extract information about the two contributions which composes the effective magnetic anisotropy field.

Keywords: Ferrite nanoparticles, Exchange bias effect, Saturation magnetization, Saturation criteria, Magnetic anisotropy

Introduction

Non-saturation of the magnetization is a recurrent problem in fine particle magnetism [1, 2, 3, 4]. When studying such systems, a key issue is ensuring that the effective anisotropy energy barrier is overcome, which leads to the correct determination of magnetic quantities, and besides, avoids misinterpretation of involved magnetic processes, allowing, for example to sort out major loop effects from minor loop ones. The overcoming of this energy barrier is what we mean by magnetic saturation.

Magnetic nanoparticles (NPs) have their anisotropy coming from different contributions [5]. The magneto-crystalline anisotropy [6] is determined by the periodic arrangement of atoms added to both exchange interactions and L-S coupling. Besides the magneto-crystalline anisotropy, the NPs also possess additional energetic contributions provided by shape and surface.

Small nanoparticles are frequently described as presenting an effective anisotropy of uniaxial symmetry [2], displaying a two-state energetic profile. These stable states are separated by an anisotropy energy barrier E_a. This barrier rules the magnetic relaxation processes, and consequently the rising of superparamagnetism (magnetic blocking).

Email address: rcabreiragomes@outlook.com (Rafael Cabreira Gomes)

Due to the spatial confinement of the magnetic system, finite size effects and surface disorder can also influence the magnetic properties [7, 8, 9] and decrease the cooperative magnetization. The existence of interface leads to undercoordinated atoms in the outer shell and uncompensated surface spins [10] with high local anisotropy [11]. In the case of ferrite NPs, [12, 13] the magnetic moments of the surface, which are canted with respect to the magnetic core [1], can be frozen for temperatures below 50 K in a disordered spin-glass like (SGL) state [14, 15]. These effects become even more important for smaller NPs, leading to the present bi-magnetic core@shell morphology composed by a ferrimagnetic (FiM) ordered core covered by an SGL disordered shell[16].

The application of an external magnetic field on such magnetic NPs can favor an energetic configuration of spins that triggers a magnetic coupling through the interface separating the different magnetic ordering. This magnetic coupling can create a unidirectional anisotropy field which adds to the uniaxial anisotropy field of the system (H_κ) and induces an horizontal displacement of the hysteresis loop [17], a phenomenon called Exchange Bias (EB)[18]. Depending on the strength of the magnetic coupling and on the consequent change in H_κ, more intense magnetic fields can be required to achieve magnetic saturation of the sample. If this requirement is not satisfied, the complete reversion of the magnetization is not achieved and the

hysteresis loop corresponds to a minor loop [19]. For instance, Kodama *et al* reported for $NiFe_2O_4$ NPs with a diameter of 6.5 nm, an horizontal shift of field cooled (FC) hysteresis loops caused by the freezing of disordered surface spins [2, 10, 14]. The authors prudently named the observed loop shift as h_{shift} due to the fact that the low temperature hysteresis loops of NPs do not close, even in intense magnetic fields (H=16 T).

In recent papers we have investigated the exchange bias effect in 3 nm sized $MFe_2O_4@\gamma$-Fe_2O_3 core@shell nanoparticles [20, 21], M being Co or Mn divalent metal ions. Such ultrasmall NPs have their magnetic properties strongly influenced by surface effects [12, 22], which hinder the magnetic saturation. In this case, in spite of the small size of the NPs, a maximum field of 9 T was sufficient to enable the observation of the EB phenomenon.

In this context, the main goal of this work is to highlight the influence of the external field strength on the magnetic measurements and consequently the interpretation of the involved magnetization processes.

We further investigate two core@shell ultrasmall NPs samples with contrasting core anisotropies cited above. These are studied in two different magnetic regimes as frozen ferrofluids and as powder samples. Here, our objective is not characterizing interaction regimes [23], but testing the saturation criteria of the magnetization loops. It's worth emphasizing that the reliability of the nature of the hysteresis loop shifts depends on the actual magnetic saturation of the sample and this issue demands the fulfillment of saturation criteria. This work will help to elucidate the relation between magnetic saturation and anisotropy by proposing complementary procedures to investigate this matter in detail.

1. Materials and Methods

1.1. Sample production and characteristics

Here, we have produced ultrasmall core@shell NPs based on $CoFe_2O_4@\gamma$-Fe_2O_3 (sample Co3) and $MnFe_2O_4@\gamma$-Fe_2O_3 (sample Mn3), by chemical synthesis route. The synthesis of such bi-magnetic nanoparticles and their water based colloidal dispersions which are electrostatically stabilized, follows a three steps procedure:

i - Firstly, the nanoparticles are obtained by polycondensation of solutions of $FeCl_3$ (1 M) and $Co(NO_3)_2$ or $MnCl_2$ (0.5 M) in a NH_4OH medium (2 M). Afterwards, the precipitate is magnetically decanted and washed with distilled water;

ii - The core@shell morphology arises from the surface treatment step, which can be separated into two other steps, the acidic washing in order to invert the surface charge and the hydrothermal treatment with an iron(III) nitrate solution (1 M), which creates an iron rich surface (γ-Fe_2O_3 shell). This maghemite shell protects the ferrite core from acidic dissolution and should modulate the NPs magnetic properties;

iii - Finally, the NPs are peptized in acidic medium (HNO_3) by adjustment of the pH which establishes the surface charge density and of the ionic strength which screens the NPs surface potential. This strategy leads to an electric double layer that prevents agglomeration of nanoparticles [24, 25];

More details about the chemical synthesis of electrostatically stabilized magnetic fluids can be found elsewhere [26, 27, 28, 29].

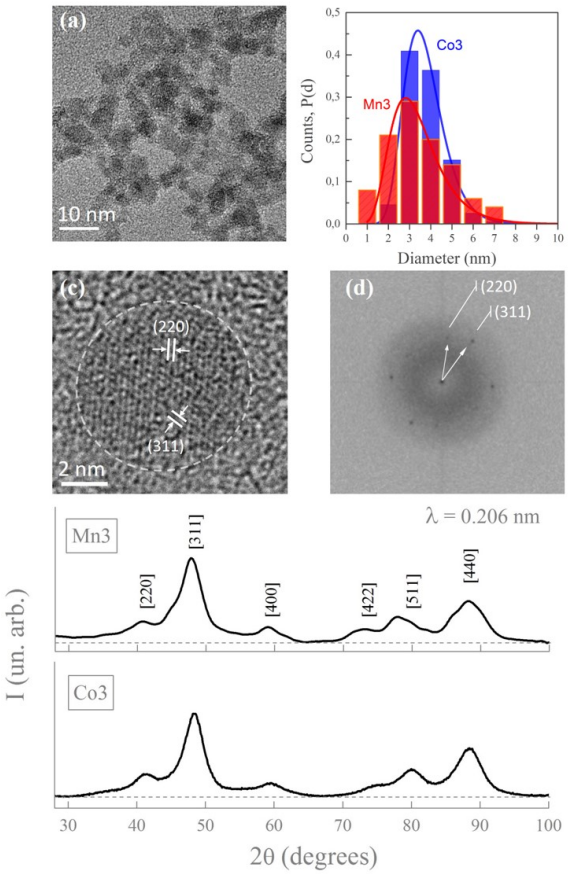

Figure 1: (a) TEM image of sample Co3, which (together with Fig. 1c) is representative for both samples. (b) Size histograms obtained from TEM images and log normal fit, results are in the table 1. (c) High Resolution TEM of Co3 sample. The crystalline planes represented on the NPs were identified by FFT depicted on the panel (d). XRD spectra of Mn3 and Co3 samples.

To determine the morphochemical composition of synthesized NPs and the volume fraction (Φ) occupied by NPs in the sample we used Atomic Absorption Spectroscopy (AAS) measurements performed using a Thermo Scientific spectrometer model S - series AA. Here, the molar fraction of divalent metals, written as,

$$\chi_M = \frac{[M^{2+}]}{[M^{2+}] + [Fe^{3+}]}, \quad (1)$$

is the key parameter to obtain information about the morphochemical composition (see table 1). A value of $\chi_M = 0.33$ indicates NPs with ferrite stoichiometry while smaller values are associated to iron rich nanoparticles. By applying the

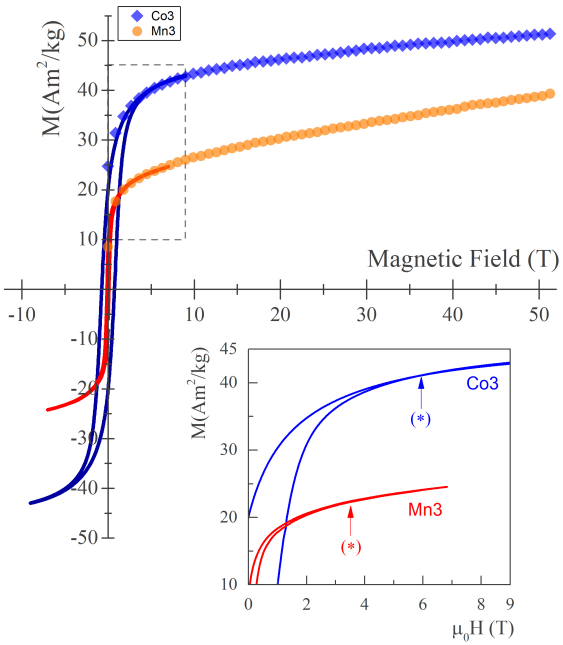

Figure 2: Magnetic measurements performed at 5K with powder samples. The solid lines are Mn3 and Co3 hysteresis loops obtained by VSM. The dots and diamonds are the downward branches of the high field hysteresis loop from LNCMI experiments. The inset shows the detail of the VSM M×H loops, with the symbol ∗ indicating the irreversible field.

core@shell model developed in [29], we found the proportions of maghemite phase collected in table 1. This method to determine the morphochemical composition of samples was confirmed in a recent paper [30] where samples synthesized by the same procedure were investigated using quantitative Scanning Transmission Electron Microscopy (STEM).

The morphostructural characterization of these samples has already been performed [20, 21, 23]. In short, the crystalline structure and the size distribution of nanoparticles were characterized by both Transmission Electron Microscopy (TEM) and X-Ray Difraction (XRD).

A summary of these results is presented in figure 1. As expected, the nanoparticles, with rock-like shape, crystallize in a spinel structure, and their size distribution is ruled by a log-normal probability density function. The median diameter (d_0) and the polydispersity (σ) obtained by fitting the size distribution histograms of both samples are presented in table 1. The mean crystalline diameter (d_X) of nanoparticles was obtained by applying the Scherrer's formula to the most intense diffraction peak of the XRD spectra. Both results are in good agreement and point out to a mean diameter around 3 nm. We have therefore named the samples Mn3 and Co3.

1.2. Magnetic measurements

The magnetic measurements were taken using two facilities. The main experiments were performed using a Quantum Design PPMS Mod. 6000 with a Vibrating Sample Magnetometer (VSM) setup; equipped with a superconducting coil which produces magnetic fields in the range of ±9 T in temperatures from 2 K to 350 K. Samples were also measured at *Laboratoire National des* Champs Magnétiques Intenses - LNCMI in Toulouse/France using 150 ms pulses of magnetic fields up to 52 T.

In the case of PPMS measurements, the Co3 and Mn3 samples have their magnetic properties investigated for both dilute ferrofluid (frozen at low T) and powder. The samples were prepared in a home made sample holder composed by two pieces of plexyglass: a tube with ~70 mm^3 of inner volume and a stopper. After filling the sample holder, the stopper is adhered to the tube with chloroformium glue. In order to remove the solvent and sample holder contributions, the signal from sample holder both empty and filled with electrolyte (HNO_3 solution with pH=2) was measured. The high magnetic fields measurements were performed only in powder samples, prepared on special sample holders provided by LNCMI.

The temperature dependence of magnetization and M×H loops were investigated for each sample by using the PPMS. To obtain the M×T curves, the sample is firstly frozen down to 5 K under zero magnetic field. Afterwards, an external field is applied ($H_{measure}$) and zero field cooling (ZFC) magnetization is obtained by warming the sample up to 250 K. Subsequently, the corresponding field cooling (FC) curve is recorded while freezing the sample under a cooling field (H_{cool}) of the same intensity as $H_{measure}$. Here, we performed these experiments using $\mu_0 H_{cool}$ between 10 mT and 6 T, being μ_0 the vacuum magnetic permeability.

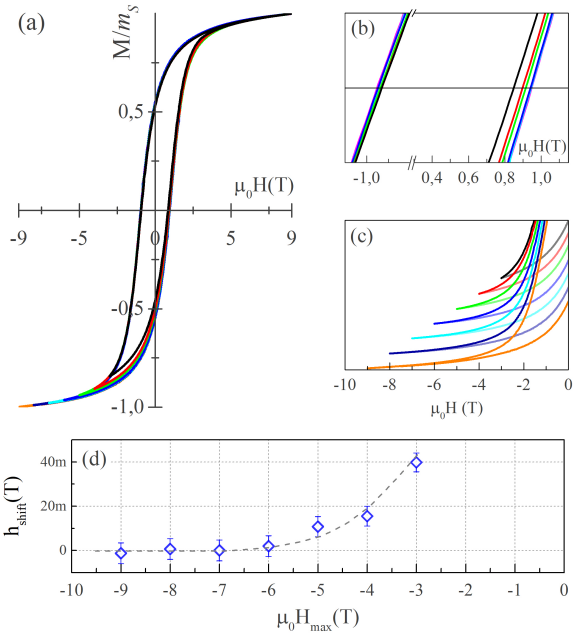

Figure 3: ZFC M×H loop of Co3 ferrofluid sample (Φ = 0.6 %) measured with different $-H_{\max}$ at 5 K. All minor loops measurements are depicted in (a) panel. (b) and (c) depict the enlarged views of the main hysteresis loops. Specially in panel (c), a gap between the curves is artificially introduced for a better view. (d) h_{shift} values resulted from the forced minor loops procedure.

All measurements of hysteresis loops were carried out at low temperatures for samples frozen by either ZFC or FC procedure. In the case of ferrofluids, before performing the FC pro-

tocol the sample is ZFC to 250 K in order to avoid magnetic texturing of sample and ensuring a random anisotropy axes distribution of NPs. It should be noted that such temperature is higher than the blocking temperatures of both types of samples, which are 50 K and 160 K (fig.4) for Mn3 and Co3, respectively.

Additionally, we have used the Forced Minor Loops (FML) procedure to investigate the saturation of ZFC and FC hysteresis magnetic loops of ferrofluids. In the case of ZFC loops we used a procedure presented in [19]. In brief words, the upper branch of hysteresis is obtained by starting from the maximum positive magnetic field available (+9 T) and afterwards each loop is measured varying the maximum field on the opposite direction ($-H_{max}$) from -1 T up to -9 T. The FC procedure, following [31], is performed starting from 5 K choosing a $H_{\rm cool}$ close to the values where the bias field ($H_{\rm exc}$) is maximum [21]. After cooling, the hysteresis loops are recorded using different $\mu_0 H_{max}$ values between ±1 T and ±9 T. Here, the positive and negative maximum fields are of the same magnitude.

In both FC and ZFC procedures, the horizontal shifts of hysteresis loops ($h_{\rm shift}$) are given by

$$h_{\rm shift} = \frac{H_C^+ + H_C^-}{2}, \qquad (2)$$

H_C^+ and H_C^- being the coercive fields deduced from the ascending and descending branches of hysteresis loop, respectively.

2. Results

The basic requirement to obtain a major hysteresis loop, and thus to reach magnetic saturation, is the overcoming of the anisotropy field by the external magnetic field ($H \geq H_\kappa$). In order to test this criterion, we carried out three kinds of magnetic measurements and their results are presented in the following.

2.1. Hysteresis loops and High field Magnetization

We first begin our investigations on ZFC hysteresis loops and high field measurements. Figure 2 is a composition of the curves obtained for powder samples at low temperature (5K) using the two different instruments. The high field experiments allowed us to record the descending branch of the M×H curve of each sample, which is then scaled by matching the overlapped regions of the high field curve and that measured using the VSM setup. It should be noted that both curves scale very well together even though the measurements are performed in different time scales i.e., in different H change rates. Despite the remarkable contrast between the magnetic anisotropy of the NP's core in the two samples, an increase of their magnetization in high magnetic fields is noted, being more pronounced in Mn3 one.

One of the most applied techniques to analyze the magnetic saturation of nanoparticles is to inspect the loop and find out the closure field, i.e, the field value H_{irr} where the two branches of the loop coincide. This is the point where the irreversible magnetization is sparkled and it represents the anisotropy field of the system. The Stoner & Wolhfarth (S&W) theory[32], suggests taking the n^{th}-derivative of magnetization with respect to the magnetic field ($\partial^n M/\partial H^n$) as a way to better assess the magnetic irreversibility, which is equivalent to determining the closure field . Depending on the symmetry of the anisotropy being probed, a singularity may become apparent [19]. We have compared the closure field from the major hysteresis loop and its first derivative, finding very similar values. Hence, we can extract H_κ directly from the major loop and the found values equal to $\mu_0 H_\kappa \sim 3.5$ T and ~ 6.0 T, for powder samples Mn3 and Co3 respectively. It should be noted that the closure field obtained for dilute ferrofluids differ only slightly from powder ones.

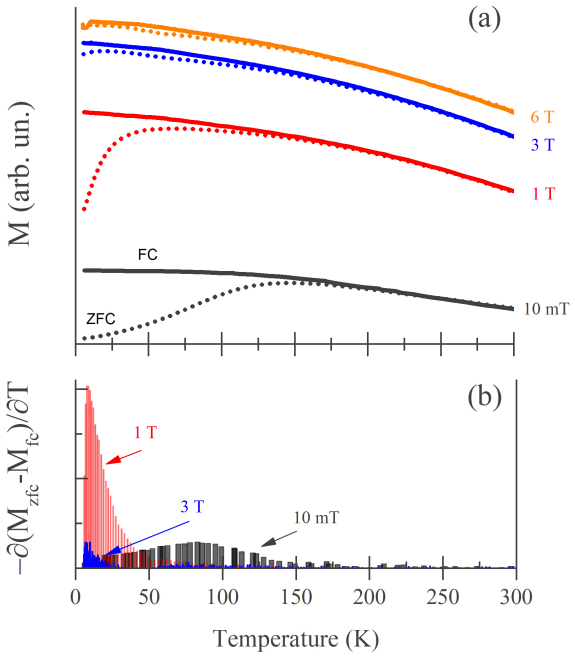

Figure 4: (a) ZFC/FC curves of Co3 powder sample in different intensities of $H_{measure}$. (b) Anisotropy Energy Profile obtained from $\partial(M_{ZFC} - M_{FC})/\partial T$ of curves.

Figure 3(a) depicts the results obtained from the ZFC FML procedure for sample Co3. In this case (highest core anisotropy) small loop shifts can be more easily detected. In panel (b), an enlarged view of the coercive field area is presented, showing that the loop shift is mainly due to the displacement of the ascending branch. Panel (c) illustrates the saturation area. The loop shift is presented in figure 3(d) and shows that h_{shift} tends to zero when the negative maximum field surpasses 6 T.

2.2. ZFC/FC DC magnetization

Following Harres *et al* [19], we propose the application of an additional procedure to confirm H_κ. The field $H_{\rm measure}$ at which the coincidence of ZFC and FC curves is achieved defines H_κ. Then, we have performed a set of ZFC-FC magnetization measurements varying $H_{\rm measure}$. Figure 4(a) shows the ZFC/FC curves for Co3 powder sample. The global feature of measurements is the displacement of the ZFC peak to lower

Table 1: Summary of samples results. The columns represent the molar fraction of divalent metal in the samples (χ_M), relative volumic fraction of maghemite shell (Φ_s/Φ), mean crystalline diameter (d_X), median diameter (d_0) and polydispersity (σ). $\mu_0 H_{irr}$ is the irreversible field or closure field, $\mu_0 H_C$ the coercive field and m_S the saturation magnetization defined as the NP magnetization at $\mu_0 H_{irr}$ (see section 3), extracted from hysteresis loops at 5 K. $\kappa_{\rm eff}$ is the (volumic) effective anisotropy constant deduced from $\kappa_{\rm eff} = \mu_0 H_{\rm irr} m_S/2$, κ_v the (volumic) core anisotropy constant deduced from $\kappa_V = \mu_0 H_C m_S/(2\zeta)$ and κ_S^{shell} the shell surface anisotropy, calculated as $\kappa_S^{shell} = d(\kappa_{\rm eff} - \kappa_v)/6$ from eqs.(3), (4) and (7) at 5K.

Sample name	χ_M	Φ_S/Φ %	d_X nm	d_0 nm	σ	$\mu_0 H_{\rm irr}$ T	$\mu_0 H_C$ T	m_S Am^2/kg	$\kappa_{\rm eff}\times10^5$ J/m^3	$\kappa_V\times10^5$ J/m^3	$\kappa_S^{shell}\times10^{-5}$ J/m^2
Mn3	0.15	0.56	3.3(4)	3.2(8)	0.3(6)	3.5(5)	0.090(4)	22.3(6)	1.96(2)	0.10(2)	8.6(4)
Co3	0.09	0.74	3.1(3)	3.3(1)	0.3(2)	6.0(1)	0.938(2)	41.2(8)	6.55(9)	2.13(1)	22(1)

temperatures when $H_{\rm measure}$ increases. This happens until approximately ~3 T and afterwards an increase of cooling field reflects in an overlap tendency of ZFC/FC curves in low temperatures region, indicating the approach to magnetic saturation.

Although the M×T curve obtained at 6T for sample Co3 scales very well to the Bloch law (fit not shown), the ZFC curve for that field possesses a small discrepancy which prevents the total overlap. At lower fields, we apply the $\partial(M_{zfc} - M_{fc})/\partial H$ procedure of [33], where the result is a profile of anisotropy energy barriers E_a involved on the magnetization process, fig.4(b). A log-normal profile of E_a is expected for a volumic anisotropy E_a. However we observed here E_a profiles with different shapes, which denotes a dependence of E_a on other factors such as temperature or chemical inhomogeneities[34].

2.3. Forced Minor Loops and Exchange bias effect

After the evaluation of magnetic saturation criteria for ZFC hysteresis loops we investigate the magnetic saturation of the sample from the FC behavior. When field cooled, these core@shell magnetic NPs present EB [18], which is quantified by the h_{shift} of the FC loop.

It has been found in Ref. [21] with loop measurements with $\mu_0 H_{max}$ = 5T for Mn3 and 9T for Co3, at 5K, that maximum horizontal loop shifts are obtained when samples Co3 and Mn3 are field cooled in ~756 mT and ~252 mT respectively. These values follow the same trend as the anisotropy field roughly evaluated in Ref. [21] by the limit of linearity of the first magnetization curve [32] in these two samples. However, when magnetic saturation is not achieved, an horizontal shift is observed and the hysteresis loop is referred as a minor one. Furthering, when a FC procedure is performed with "positive" $H_{\rm cool}$, the saturated M×H loop demonstrates a displacement of H_C^-. On the contrary, when a sample is not magnetically saturated, the FC procedure induces a false EB where the horizontal displacement is observed on H_C^+. Thus, in order to enlighten the issue of magnetic saturation we propose the FML procedure, where values of EB deduced from major loops are used as a tool to determine H_{irr}.

By analyzing the FML curves (fig.5(a)) one can evidence two important features: (*i*) the progressive increasing of $H_{\rm max}$ slightly modifies the squareness of the loop, as long as $H_{\rm max} <$

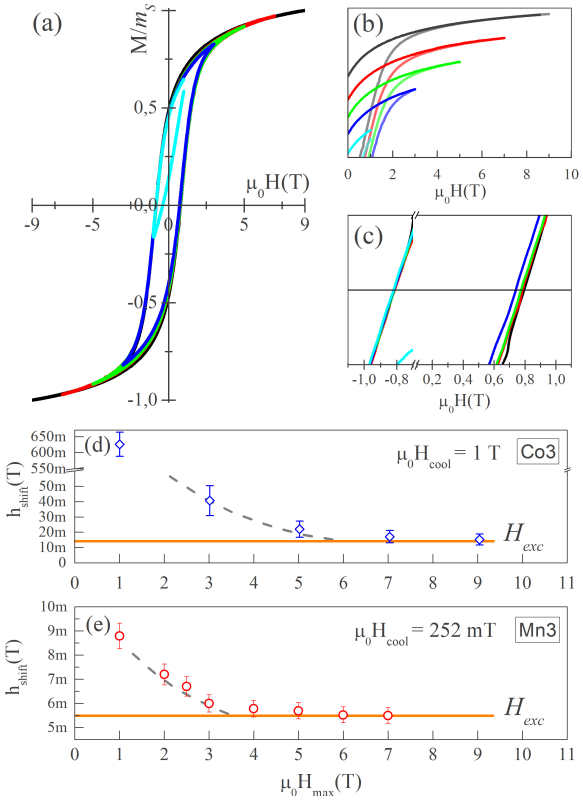

Figure 5: (a) FC M×H loop of Co3 ferrofluid sample (Φ = 0.6 %) measured with different $\pm H_{\rm max}$ at 5 K with $\mu_0 H_{cool}$ = 1T. Panels (b) and (c) give the enlarged views of main hysteresis loop. The curves in (d) and (e) show the approach $H_{\rm exc}$ with the increase of the maximum applied field ($H_{\rm max}$) used for the ferrofluid samples Co3 (Φ = 0.6 %) and Mn3 (Φ = 0.4 %). The shaded area represents the closure field.

$H_{\rm irr}$, an open hysteresis loop is obtained; (*ii*) the increase of $H_{\rm max}$ induces a reduction of h_{shift} towards an asymptotic value correspondent to the actual EB field value.

The results of h_{shift} for both samples, Co3 and Mn3 ferrofluids, are depicted in fig. 5(d,e) where $h_{\rm shift}$ is plotted as a function of the modulus of $\mu_0 H_{\rm max}$. As the curves are obtained after a FC procedure, one expects that the horizontal shift become the actual EB field value when the sample achieves magnetic saturation. In fact, the magnetic saturation is observed in M×H loops when $\pm\mu_0 H_{max} \geq \pm 3.5$ T for Mn3 sample and $\pm\mu_0 H_{max} \geq \pm 6.0$

T for Co3 sample.

Indeed if the loop of Co3 sample is measured with $\mu_0 H_{\max} = \pm 5$ T, it presents a variation about 6% between coercive field branches, which yield an $h_{\text{shift}} \approx 21$ mT, greater than the magnitude of the actual EB found for this sample in fig. 5(d) and in [20, 21].

3. Discussion

In bulk materials, the spontaneous magnetization is a physical quantity which depends exclusively on the chemical composition and crystalline structure of the material. On the other hand, on the nanoscale, the high-field magnetization of materials becomes size dependent, being influenced by phenomena such as surface disorder and finite size effects. Both effects are more pronounced in ultrasmall nanoparticles offering difficulty to achieve the saturation of magnetization [12].

In our samples, the ferrimagnetic core is surrounded by a magnetically disordered shell with uncompensated surface spins. Magnetic non-colinearity may occur even in very intense magnetic fields depending on the energy configuration of these spins, which contributes to the effective anisotropy due to intense local anisotropy fields.

In bulk materials, the saturation of sample's magnetization is evidenced by a *plateau* in the region of high fields of M×H loop. In the case of the investigated samples, whatever the magnetic nature of the core (soft or hard ferrite), an increase of magnetization is observed even in very intense fields (see fig.2). However, magnetization values measured at fields greater than the closure field limit are only related to the reversible reorientation of spins from the shell of the NPs. In this context, we define here the m_S values of both samples as the magnetization at the closure field H_{irr}. They are given in table 1. It is worth noting that Co3 sample possess a higher saturation magnetization value than Mn3, in contrast to what would be expected for the respective bulk ferrites [5, 35, 36]. This effect is most likely related to the interplay between surface disorder[37], core anisotropy[38], cation distribution[39, 40] and mixed valence states[41].

Moreover, fig.3 clearly indicates h_{shift} values of ZFC loops saturating to zero for fields higher than 3.5 and 6.0 T for Mn3 and Co3 samples, respectively, showing that beyond these values the loops correspond to a major one. The closure field is interpreted as the point where all anisotropy energy barriers are surpassed by the Zeeman energy and above this threshold, the magnetization is reversible. Under this interpretation, the closure field can be considered an effective anisotropy field $\mu_0 H_\kappa$ felt in high fields.

This field $\mu_0 H_\kappa$ can be expressed by the relation provided in S&W theory:

$$\mu_0 H_\kappa = \mu_0 H_{\text{irr}} = \frac{2E_a^{\text{eff}}}{m_S V}, \tag{3}$$

$\mu_0 H_{\text{irr}}$ being linked to the effective anisotropy E_a^{eff} of the NP and V its volume.

Furthering, one can make use of the coercive field to estimate the core anisotropy E_a^{core} of NPs by using

$$\mu_0 H_C = \zeta \mu_0 H_a = \zeta \frac{2E_a^{\text{core}}}{m_S V}, \tag{4}$$

where H_a is the core anisotropy field of the magnetic moment $m_S V$ in low fields and ζ is a coefficient which depends both on the anisotropy symmetry and the orientation distribution of the sample's anisotropy axes. In the case of a randomly oriented ensemble of non-interacting uniaxial single domain particles, the ζ-coefficient is equal to 0.48.

The results presented on Table 1 show that the two samples possess very contrasting H_C (see fig.2), as expected due to the different core ferrite (hard or soft) coming from the chemical composition of the samples.

For magnetic nanoparticles, E_a^{core} has been analyzed in the literature [42, 43], as either coming from a volume contribution [23, 44, 45, 46, 47]:

$$E_a^{core} = \kappa_V V \tag{5}$$

or from a surfacic one [3, 21, 22, 43, 48, 49]:

$$E_a^{core} = \kappa_S S. \tag{6}$$

These two formulations are equivalent with $\kappa_S = 3\kappa V/d$. An analysis as a function of d as in [22, 50] would be the only way to distinguish between these two formulations.

From the point of view of an analysis of E_a^{core} in terms of volume anisotropy (eq.(5)), they are in good agreement with the literature. For Mn-ferrite, the reference value of the anisotropy constant obtained at low temperature is $\kappa_V \sim 6 \times 10^4$ J/m^3 [44, 45] for NPs of ~7 nm diameter, slightly larger than our value of $\sim 1 \times 10^4$ J/m^3 in table 3. In the case of Co ones, the magnetic anisotropy at low temperature has been found to be between 1×10^5 J/m^3 $\leq \kappa_V \leq 3 \times 10^6$ J/m^3 for NPs of 3 nm [23, 46, 47], in agreement with the value 2.1×10^5 J/m^3 found here.

An analysis in terms of surface anisotropy of E_a^{core} (eq.(6)), would lead here to $\kappa_S = 2.1 \times 10^{-4}$ J/m^2 for Co3, of the same order as the value $\sim 10^{-4}$ J/m^2 deduced in [21] from first magnetization curves for Co3 and rather close to values found for Ni ferrites NPs (1.2×10^{-4} J/m^2 found in [51] by an optical birefringence technique and 2.5×10^{-4} J/m^2 found in [22] by under-field Mossbauer experiments). For Mn3, it would lead to $\kappa_S \sim \times 10^{-5}$ J/m^2 (slightly smaller but comparable to the values found by FerroMagnetic Resonance at 9 GHz $\kappa_S \sim 3 \times 10^{-5}$ J/m^2 for Mn3 in [48] and $\kappa_S = 2.7 \times 10^{-5}$ J/m^2 for maghemite of size 4 to 10 nm in [50, 49, 52, 43]). It is worth to note that for what concerns the quantification of surface anisotropy, most of the techniques commonly applied have a dynamic nature [48, 50, 22, 51]. In these kinds of measurements, NPs with low anisotropy are usually investigated at fields of the order of 0.33 T. However a field of up to 12 T was used in [22] for Ni ferrite, which presents a sensibly larger anisotropy.

The difference between values of H_{irr} and H_a points out to an additional anisotropic contribution in higher fields, which is here attributed to a surface anisotropy contribution, i.e., E_{eff} is

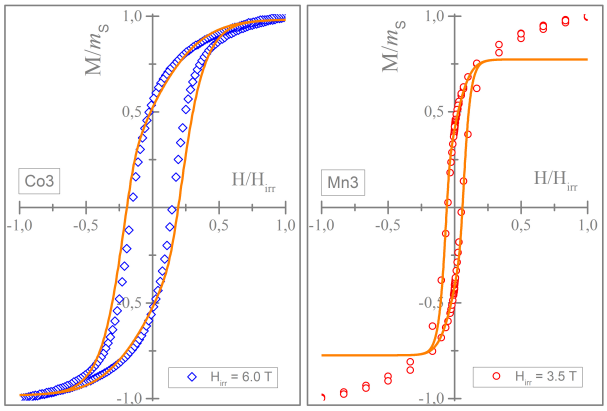

Figure 6: Absolute hysteresis loop of Co3 ferrofluid sample (blue diamonds), Mn3 ferrofluid sample (red circles) and the calculations (solid line).

a composition of core and shell magnetic anisotropies. Assuming they are additive, they would write:

$$E_a^{\text{eff}} = E_a^{\text{core}} + E_a^{\text{shell}} = E_a^{\text{core}} + \kappa_S^{shell} S. \quad (7)$$

It is worth emphasizing the remarkable agreement between the value of effective anisotropy field extracted from the closure field and from the ZFC/FC curves, which are well overlapped for cooling fields above H_κ (see Fig. 4).

The FML protocol shows that the value of $H_{\max}$ required to stabilize the horizontal shift due to the actual EB field is also well compatible with $H_\kappa = H_{irr}$.

Finally, in order to test if these obtained values represent the anisotropy field of the NPs and consequently if they are magnetically saturated in ZFC and FC regimes above those fields, we performed a calculation of hysteresis loops by using the S&W theory[32]. We consider a polydisperse ensemble of randomly oriented non-interacting single domain particles, each particle presenting the same uniaxial anisotropy $E_a^{core} = \kappa_V V$. This assumption is based on the experimental values for the squareness of the ZFC hysteresis loops, which are compatible with a uniaxial anisotropy.

For the calculation, each NP contribution is volume weighted considering the log-normal distribution parameters shown in Table 1. As can be seen in fig.6, we found a good agreement between the calculations (solid line) and the experimental data for both samples in the low field region, as expected. The normalization of the curves in field axis, calls attention for the ratio $\frac{H_{irr}}{H_C}$, which is 5 times greater for Mn3 sample as compared to Co3. This can be related to the more pronounced influence of surface anisotropy in the Mn3 sample, in agreement with the paramagnetic like magnetization increase we observe in the high field experiments. Thus, the discrepancy between the calculations and the experimental data in higher fields may be explained by the surface anisotropy energy, which is not taken into account in the calculations.

4. Conclusion

In this paper we investigate the magnetic saturation criteria of 3 nm-sized nanoparticles and their relation with both anisotropy and exchange bias fields. Due to the confinement at nanoscale, the saturation of ultrasmall particles magnetization is not always possible at H-intensities available in conventional magnetometers since the effective anisotropy field might not be overcome. By using different procedures, we showed that the increment of magnetization observed on high intensity magnetic fields, up to 52 T, does not represent the non-overcome of the anisotropy barrier but a contribution arising from some surface spins able to rotate reversibly with the applied field. The samples can be considered to be completely magnetized when the two branches of hysteresis loops are overlapped. The closure field is related to the effective anisotropy of the samples which is the sum of two contributions. One arises from the core and is probed here by the coercive field at low temperatures. The additional contribution comes mainly from the disordered surface, which can only be observed in high fields.

The effective anisotropy field determined from the closure fields is in good agreement with that needed to get a full overlapping of ZFC and FC magnetization curves. Also, the obtained values are corroborated by both ZFC and FC forced minor loops protocols, which show a complete saturation for fields above the irreversibility. By using the core anisotropy constant extracted from the coercivity and the saturation magnetization obtained at the closure field, we obtain a calculated hysteresis loop that matches the low temperature experimental data, with the exception of the high field surface contribution.

Our results help to elucidate the issues regarding magnetic saturation and propose complementary paths to analyze and verify its relation with the anisotropy fields in ultrasmall bimagnetic nanoparticles. In the future, analyzing the field range above the closure field would help to enlighten the role and the mechanism of surface disorder, anisotropy and magnetization.

Acknowledgements

We thank EMFL-LNCMI Toulouse for experimental time allocation (Proposal EuroMagnet GSO27-210) and G. Ballon - LNCMI - Toulouse. Authors gratefully acknowledge the financial support of the Brazilian agencies CAPES, CNPq (Grants 465259/2014-6, 202340/2015-5, 400849/2016-0, 305796/2016-0 and 422740/2018-7), INCT-FCx (Grant 2014/50983-3) and FAP-DF (Grants 0193.001569/2017 and 0193.001376/2016).

References

References

[1] J. M. D. Coey, Noncollinear Spin Arrangement in Ultrafine Ferrimagnetic Crystallites, Physical Review Letters 27 (1971) 1140–1142.
[2] R. H. Kodama, A. E. Berkowitz, E. J. McNiff, Jr., S. Foner, Surface Spin Disorder in $NiFe_2O_4$ Nanoparticles, Physical Review Letters 77 (1996) 394–397.
[3] J. Dormann, D. Fiorani, Magnetic Properties of Fine Particles, ISSN, Elsevier Science, 2012.
[4] D. Fiorani, Surface effects in magnetic nanoparticles, Springer Science & Business Media, 2005.
[5] B. D. Cullity, C. D. Graham, Introduction to magnetic materials, volume 12, IEEE/Wiley, 2009.

[6] J. I. Martín, J. Nogués, K. Liu, J. L. Vicent, I. K. Schuller, Ordered magnetic nanostructures: Fabrication and properties, Journal of Magnetism and Magnetic Materials 256 (2003) 449–501.

[7] X. Batlle, A. Labarta, Finite-size effects in fine particles: magnetic and transport properties, Journal of Physics D: Applied Physics 35 (2002) R15–R42.

[8] C. R. Alves, R. Aquino, M. Sousa, H. R. Rechenberg, G. F. Goya, F. Tourinho, J. Depeyrot, Low Temperature Experimental Investigation of Finite-Size and Surface Effects in $CuFe_2O_4$ Nanoparticles of Ferrofluids, Journal of Metastable and Nanocrystalline Materials 20-21 (2004) 694–699.

[9] F. G. d. Silva, J. Depeyrot, A. F. C. Campos, R. Aquino, D. Fiorani, D. Peddis, Structural and magnetic properties of spinel ferrite nanoparticles, Journal of Nanoscience and Nanotechnology 19 (2019) 4888–4902.

[10] R. H. Kodama, A. E. Berkowitz, Atomic-scale magnetic modeling of oxide nanoparticles, Physical Review B 59 (1999) 6321–6336.

[11] M. Vasilakaki, K. N. Trohidou, Numerical study of the exchange-bias effect in nanoparticles with ferromagnetic core/ferrimagnetic disordered shell morphology, Phys. Rev. B 79 (2009) 144402.

[12] R. Aquino, J. Depeyrot, M. H. Sousa, F. A. Tourinho, E. Dubois, R. Perzynski, Magnetization temperature dependence and freezing of surface spins in magnetic fluids based on ferrite nanoparticles, Physical Review B 72 (2005) 184435.

[13] P. V. Hendriksen, S. Linderoth, P.-A. Lindgård, Finite-size modifications of the magnetic properties of clusters, Phys. Rev. B 48 (1993) 7259–7273.

[14] R. Kodama, A. Berkowitz, Surface-Driven Effects on the Magnetic Behavior of Oxide Nanoparticles, Surface Effects in Magnetic Nanoparticles (2005) 189–216.

[15] M. Estrader, A. López-Ortega, S. Estradé, I. Golosovsky, G. Salazar-Alvarez, M. Vasilakaki, K. Trohidou, M. Varela, D. Stanley, M. Sinko, et al., Robust antiferromagnetic coupling in hard-soft bi-magnetic core/shell nanoparticles, Nature communications 4 (2013) 2960.

[16] J. Nogués, J. Sort, V. Langlais, V. Skumryev, S. Suriñach, J. S. Muñoz, M. D. Baró, Exchange bias in nanostructures, Physics Reports 422 (2005) 65–117.

[17] J. Nogués, I. K. Schuller, Exchange bias, Journal of Magnetism and Magnetic Materials 192 (1999) 203–232.

[18] W. H. Meiklejohn, C. P. Bean, New Magnetic Anisotropy, Physical Review 102 (1956) 1413–1414.

[19] A. Harres, M. Mikhov, V. Skumryev, A. M. H. De Andrade, J. E. Schmidt, J. Geshev, Criteria for saturated magnetization loop, Journal of Magnetism and Magnetic Materials 402 (2016) 76–82.

[20] F. G. Silva, R. Aquino, F. A. Tourinho, V. I. Stepanov, Y. L. Raikher, R. Perzynski, J. Depeyrot, The role of magnetic interactions in exchange bias properties of $MnFe_2O_4@\gamma$-Fe_2O_3 core/shell nanoparticles, Journal of Physics D: Applied Physics 46 (2013) 285003.

[21] R. Cabreira-Gomes, F. G. Silva, R. Aquino, P. Bonville, F. Tourinho, R. Perzynski, J. Depeyrot, Exchange bias of $MnFe_2O_4@\gamma$-Fe_2O_3 and $CoFe_2O_4@\gamma$-$Fe2O_3$ core/shell nanoparticles, Journal of Magnetism and Magnetic Materials 368 (2014) 409–414.

[22] E. C. Sousa, H. R. Rechenberg, J. Depeyrot, J. A. Gomes, R. Aquino, F. A. Tourinho, V. Dupuis, R. Perzynski, In-field Mossbauer study of disordered surface spins in core/shell ferrite nanoparticles, Journal of Applied Physics 106 (2009) 093901.

[23] C. A. M. Vieira, R. Cabreira-Gomes, F. G. Silva, A. L. Dias, R. Aquino, A. F. C. Campos, J. Depeyrot, Blocking and remanence properties of weakly and highly interactive cobalt ferrite based nanoparticles, Journal of Physics: Condensed Matter 31 (2019) 175801.

[24] J. Israelachvili, Intermolecular and Surface forces, 1985, Academic Press, 2011.

[25] F. Tourinho, J. Depeyrot, G. d. Silva, M. Lara, Electric double layered magnetic fluids (edl-mf) based on spinel ferrite nanostructures $[(m^{+2}_{1-x}fe^{+3}_{x})]_a[(fe^{+3}_{2-x}m^{+2}_{x})]_b o^{-2}_4$, Brazilian Journal of Physics 28 (1998) 00 – 00.

[26] R. Aquino, F. A. Tourinho, R. Itri, M. C. F. L. E Lara, J. Depeyrot, Size control of $MnFe_2O_4$ nanoparticles in electric double layered magnetic fluid synthesis, Journal of Magnetism and Magnetic Materials 252 (2002) 23–25.

[27] F. A. Tourinho, R. Franck, R. Massart, Aqueous ferrofluids based on manganese and cobalt ferrites, Journal of Materials Science 25 (1990) 3249–3254.

[28] M. H. Sousa, F. A. Tourinho, J. Depeyrot, G. J. da Silva, M. C. F. L. Lara, New Electric Double-Layered Magnetic Fluids Based on Copper, Nickel, and Zinc Ferrite Nanostructures, The Journal of Physical Chemistry B 105 (2001) 1168–1175.

[29] J. D. A. Gomes, M. H. Sousa, F. A. Tourinho, R. Aquino, G. J. Da Silva, J. Depeyrot, E. Dubois, R. Perzynski, Synthesis of core-shell ferrite nanoparticles for ferrofluids: Chemical and magnetic analysis, Journal of Physical Chemistry C 112 (2008) 6220–6227.

[30] V. Pilati, R. Cabreira Gomes, G. Gomide, P. Coppola, F. G. Silva, F. L. O. Paula, R. Perzynski, G. F. Goya, R. Aquino, J. Depeyrot, Core/shell nanoparticles of non-stoichiometric zn–mn and zn–co ferrites as thermosensitive heat sources for magnetic fluid hyperthermia, The Journal of Physical Chemistry C 122 (2018) 3028–3038.

[31] G. Salazar-Alvarez, J. Sort, S. Suriñach, M. D. Baró, J. Nogués, Synthesis and size-dependent exchange bias in inverted coreshell mno—mn_3o_4 nanoparticles, Journal of the American Chemical Society 129 (2007) 9102–9108.

[32] E. C. Stoner, E. P. Wohlfarth, A Mechanism of Magnetic Hysteresis in Heterogeneous Alloys, Philosophical Transactions of the Royal Society A: Mathematical, Physical and Engineering Sciences 240 (1948) 599–642.

[33] J. S. Micha, B. Dieny, J. R. Régnard, J. F. Jacquot, J. Sort, Estimation of the Co nanoparticles size by magnetic measurements in Co/SiO2discontinuous multilayers, Journal of Magnetism and Magnetic Materials 272-276 (2004) 2003–2004.

[34] H. Callen, E. Callen, The present status of the temperature dependence of magnetocrystalline anisotropy, and the l(l+1)2 power law, Journal of Physics and Chemistry of Solids 27 (1966) 1271 – 1285.

[35] S. Chikazumi, Physics of Ferromagnetism, Oxford University Press on Demand, 1997.

[36] J. Smit, H. Wijn, Ferrites, philips technical library, Eindhoven, The Netherlands 278 (1959).

[37] R. Kodama, A. Berkowitz, E. McNiff Jr, S. Foner, Surface spin disorder in ferrite nanoparticles, Journal of Applied Physics 81 (1997) 5552–5557.

[38] X. Batlle, N. Pérez, P. Guardia, O. Iglesias, A. Labarta, F. Bartolomé, L. M. Garca, J. Bartolomé, A. G. Roca, M. P. Morales, C. J. Serna, Magnetic nanoparticles with bulklike properties (invited), Journal of Applied Physics 109 (2011) 1–7.

[39] D. Peddis, N. Yaacoub, M. Ferretti, A. Martinelli, G. Piccaluga, A. Musinu, C. Cannas, G. Navarra, J. Greneche, D. Fiorani, Cationic distribution and spin canting in cofe2o4 nanoparticles, Journal of Physics: Condensed Matter 23 (2011) 426004.

[40] J. Gomes, G. Azevedo, J. Depeyrot, J. Mestnik-Filho, F. Paula, F. Tourinho, R. Perzynski, Structural, chemical, and magnetic investigations of core–shell zinc ferrite nanoparticles, The Journal of Physical Chemistry C 116 (2012) 24281–24291.

[41] F. H. Martins, F. G. Silva, F. L. Paula, J. de A. Gomes, R. Aquino, J. Mestnik-Filho, P. Bonville, F. Porcher, R. Perzynski, J. Depeyrot, Local structure of core–shell mnfe2o4+ δ-based nanocrystals: Cation distribution and valence states of manganese ions, The Journal of Physical Chemistry C 121 (2017) 8982–8991.

[42] J. L. Dormann, D. Fiorani, E. Tronc, Magnetic Relaxation in Fine-Particle Systems, John Wiley Sons, Ltd, pp. 283–494.

[43] R. Perzynski, Y. L. Raikher, Effect of surface anisotropy on the magnetic resonance properties of nanosize ferroparticles, in: Surface effects in magnetic nanoparticles, Springer, 2005, pp. 141–187.

[44] A. J. Rondinone, C. Liu, Z. J. Zhang, Determination of magnetic anisotropy distribution and anisotropy constant of manganese spinel ferrite nanoparticles, The Journal of Physical Chemistry B 105 (2001) 7967–7971.

[45] S. Yoon, K. M. Krishnan, Temperature dependence of magnetic anisotropy constant in manganese ferrite nanoparticles at low temperature, Journal of Applied Physics 109 (2011) 07B534.

[46] D. Peddis, M. V. Mansilla, S. Mørup, C. Cannas, A. Musinu, G. Piccaluga, F. D'Orazio, F. Lucari, D. Fiorani, Spin-Canting and Magnetic Anisotropy in Ultrasmall $CoFe_2O_4$ Nanoparticles, The Journal of Physical Chemistry B 112 (2008) 8507–8513.

[47] A. T. Ngo, P. Bonville, M. P. Pileni, Spin canting and size effects in nanoparticles of nonstoichiometric cobalt ferrite, Journal of Applied Physics 89 (2001) 3370–3376.

[48] F. G. da Silva, "Propriedades magneticas, desordem de superficie e polarizaao por intercâmbio de nanoparticulas magneticas", Ph.D. thesis,

Universidade de Brasilia/Universite Pierre et Marie Curie, 2013.
[49] V. P. Shilov, J.-C. Bacri, F. Gazeau, F. Gendron, R. Perzynski, Y. L. Raikher, Ferromagnetic resonance in ferrite nanoparticles with uniaxial surface anisotropy, Journal of Applied Physics 85 (1999) 6642–6647.
[50] F. Gazeau, J. Bacri, F. Gendron, R. Perzynski, Y. Raikher, V. Stepanov, E. Dubois, Magnetic resonance of ferrite nanoparticles: evidence of surface effects, Journal of Magnetism and Magnetic Materials 186 (1998) 175 – 187.
[51] Y. L. Raikher, V. I. Stepanov, J. Depeyrot, M. H. Sousa, F. A. Tourinho, E. Hasmonay, R. Perzynski, Dynamic optical probing of the magnetic anisotropy of nickel-ferrite nanoparticles, Journal of Applied Physics 96 (2004) 5226–5233.
[52] D. Fiorani, Surface effects in magnetic nanoparticles, Springer Science & Business Media, 2005.